

# Sub-Rayleigh lithography using high flux loss-resistant entangled states of light

Shamir Rosen, Itai Afek, Yonatan Israel, Oron Ambar, Yaron Silberberg<sup>1</sup>

<sup>1</sup>*Department of Physics of Complex Systems, Weizmann Institute of Science, Rehovot, Israel*

Quantum lithography achieves phase super-resolution using fragile, experimentally challenging entangled states of light. We propose a scalable scheme for creating features narrower than classically achievable, with reduced use of quantum resources and consequently enhanced resistance to loss. The scheme is an implementation of interferometric lithography using a mixture of an SPDC entangled state with intense classical coherent light. We measure coincidences of up to four photons mimicking multiphoton absorption. The results show a narrowing of the interference fringes of up to 30% with respect to the best analogous classical scheme using only 10% of the non-classical light required for creating NOON states.

PACS numbers: 42.50.St 42.50.Dv

*Introduction.* Quantum entanglement has been shown to be instrumental in surpassing the classical limits in various technological fields [1]. In the case of optical lithography, it has been proposed that multi-photon entanglement can be harnessed to generate arbitrary patterns with a higher resolution than that attainable with classical light [2–4]. Specifically, in the technique of interferometric lithography proposed by Boto et. al [2], a prescribed pattern is written periodically on a multi-photon absorbing substrate via interference between two intersecting beams. The entangled states most often associated with quantum lithography are the so called ‘high-NOON’ states, which are path-entangled Fock states with  $N$ -photons in either one of two paths [5, 6]. Such states collect phase  $N$  times faster than classical light, hence their super-resolution capabilities. Indeed, efforts to generate high-NOON states have been reported over the last decade [7–10], striving for larger  $N$  values.

In interferometric lithography the minimal feature size is determined by the minimal width that can be written with an interference pattern, hence the drive to form narrower fringes. A Mach-Zehnder interferometer is prototypical for studying such interferences. While a classical source with a standard intensity detector will show a bright fringe half a wavelength wide, it is possible to use  $N$ -photon absorption (or, alternatively, an  $N$ -photon detector) to get a  $\sqrt{N}$  narrower feature, still using a classical source. In contrast, using such detectors with a perfect  $N$ -photon NOON state would generate fringes that are  $N$  times narrower. The additional  $\sqrt{N}$  narrowing due to the entanglement of the light is a purely quantum effect.

Although NOON states possess exceptional super-resolution capabilities, they are limited by heavy experimental constraints. All schemes for generating high-NOON states use nonclassical light sources such as spontaneous parametric down-converted (SPDC) light as a resource for entanglement. For example, Fig.1(A) shows schematically our approach, where an SPDC beam is mixed on a beamsplitter with a coherent state to form an almost perfect superposition of NOON states [10, 11].

It is the brightness of the nonclassical source that poses the main limitation in such systems, and it is important to find ways to minimize the use of this resource.

Another experimental difficulty that comes hand-in-hand with the quantum nature of the light is an exceptionally high sensitivity to loss. NOON states in particular are  $N$  times more sensitive to loss compared to classical pulses. This optical loss is practically unavoidable as it is inherent to most optical elements as well as to any detection system.

One possible path towards overcoming these difficulties is the use of partially entangled states. Such states have recently been used to achieve optimal sensitivity in phase measurements [12]. Here we introduce and generate a set of partially entangled states designed for use in super-resolution lithography. We show theoretically and demonstrate experimentally, that when an SPDC beam is mixed in with a coherent state, significant narrowing of the  $N$ -photon fringe occurs with significantly less SPDC than required for forming a NOON state. Therefore, quantum resolution enhancement can be obtained with reduced demand on the quantum resources. Moreover, we show that the reduced use of SPDC enables a major increase in the generating flux leading to high multiphoton absorption rates, even in the presence of high losses. Another benefit we discovered is that these high flux loss-resistant entangled states exhibit just one major fringe per wavelength, whereas the other fringes that would appear in a NOON state reduce in magnitude and hence will be easier to eliminate.

We note that another approach towards raising the quantum flux used an unseeded OPA as the source of entangled photons. This scheme however is limited to doubling the density of the interference fringes [13, 14].

*Theoretical analysis.* We present here a detailed analysis of a general two-mode entangled state created by mixing SPDC with a coherent state and compute its interference pattern in a Mach Zehnder interferometer. We find the dependence of the width of the interference fringes on the parameters of the two input modes, and observe that minute amounts of SPDC account for most of the

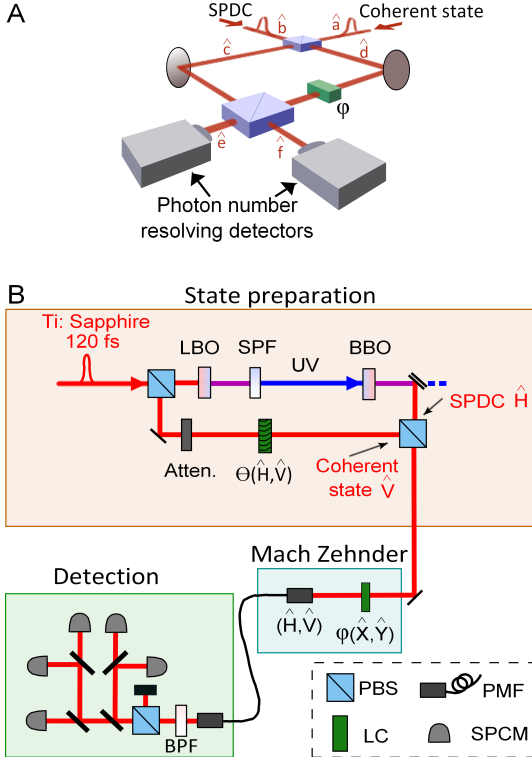


Figure 1: (color online). Experimental Setup. (A) Illustration of the generation of the loss-resistant states in a Mach Zehnder (MZ) interferometer fed by a coherent state and SPDC. The loss-resistant states are created in modes  $\hat{c}$  and  $\hat{d}$  of the MZ and are subsequently interfered and measured in a photon number resolving apparatus. (B) Detailed layout of the setup. 120-fs pulses from a Ti:sapphire oscillator operated at 80 MHz are up-converted using a 2.74-mm lithium triborate (LBO) crystal, short pass filtered, and then down-converted using a 1.78-mm beta barium borate (BBO) crystal, creating correlated photon pairs at the original wavelength (808 nm). This SPDC ( $\hat{H}$  polarization) is mixed with attenuated coherent light ( $\hat{V}$  polarization) on a polarizing beamsplitter (PBS). A thermally induced drift in the relative phase is corrected every few minutes with the use of a liquid crystal (LC) phase retarder. The MZ is polarization-based in a collinear inherently phase-stable design. The MZ phase is controlled using an additional LC phase retarder at  $45^\circ$ , which adjusts the phase between  $\hat{X}$  and  $\hat{Y}$  polarizations. The spatial and spectral modes are matched using a polarization-maintaining fiber (PMF) and a 3-nm (full width at half max) bandpass filter (BPF). Photon number-resolving detection is performed using an array of single-photon counting modules (SPCM, Perkin Elmer).

fringe narrowing. Consider the setup of Fig.1(A) where a Mach-Zehnder (MZ) interferometer is fed by a coherent state,  $|\alpha\rangle_a$ , and SPDC,  $|\xi\rangle_b$ , in its input ports. The lower path amplitude accumulates a controllable phase shift  $\varphi$  before the two modes interfere. Rather than interfering on an absorbing substrate as originally suggested, modes  $\hat{c}$  and  $\hat{d}$  impinge on two ports of a second beamsplitter and are subsequently detected by photon number resolv-

ing detectors **e** and **f**. The event  $|0, N\rangle_{e,f}$  is equivalent to an N-photon absorption event [2].

The input state can be written as

$$|\psi\rangle_{a,b} = |\alpha\rangle_a \otimes |\xi\rangle_b \quad (1)$$

where  $\alpha$  is a coherent state defined by:

$$|\alpha\rangle = \sum_{n=0}^{\infty} \exp(-\frac{1}{2}|\alpha|^2) \frac{\alpha^n}{\sqrt{n!}} |n\rangle, \quad (2)$$

$$\alpha = |\alpha| \exp(i\theta_{cs}) \quad (3)$$

and  $\xi$  is single mode degenerate SPDC with the following wave function[1]:

$$|\xi\rangle = \frac{1}{\sqrt{\cosh r}} \sum_{m=0}^{\infty} (-1)^m \frac{\sqrt{(2m)!}}{2^m m!} (\tanh r)^m |2m\rangle \quad (4)$$

The controllable parameters are the amplitudes of the two input modes, and the relative phase between them. We denote the pair amplitude ratio of the coherent state and SPDC inputs  $\gamma \equiv |\alpha|^2/r$  (in the limit  $r, |\alpha| \ll 1$ ) [10]. The pair amplitude ratio  $\gamma$  reflects the relative intensity of the two input states; for a given coherent state, a smaller value of  $\gamma$  reflects stronger SPDC component hence more quantum resource.

We consider N-photon absorption, which, for a given state, has a probability of  $|\langle 0, N | \psi \rangle_{e,f}|^2$ . When the loss can be neglected, the system conserves the total number of photons in the two-mode state. This means that only input states with a total number of N photons contribute to the N photon signal. We treat the subspace of N=3 as an instructive example. The input state, before the first BS is:

$$|\psi_3\rangle_{a,b} = \frac{\alpha^2}{\sqrt{6}} |3, 0\rangle_{a,b} - \frac{\alpha r}{\sqrt{2}} |1, 2\rangle_{a,b} \quad (5)$$

Under the transformation of the first BS this becomes:

$$|\psi_3\rangle_{c,d} = \frac{\alpha}{4} \left( \frac{\alpha^2 - 3r}{\sqrt{3}} (|3, 0\rangle_{c,d} + |0, 3\rangle_{c,d}) + (\alpha^2 + r) (|2, 1\rangle_{c,d} + |1, 2\rangle_{c,d}) \right) \quad (6)$$

Note that the choice of  $\alpha^2 = -r$  would generate a perfect NOON state; we continue to consider the general case. When passing through a phase shifter (PS), number states collect a phase that is equal to the PS phase,  $\varphi$ , multiplied by the number of photons in the state. Explicitly:

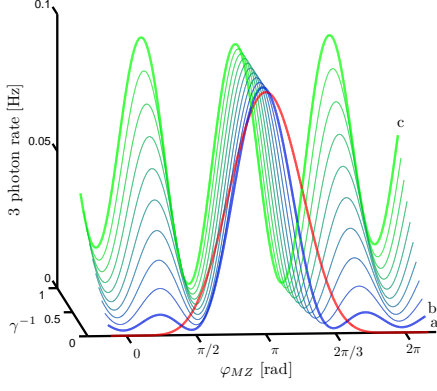


Figure 2: (color online). Simulation of 3-photon coincidence rate for  $\gamma^{-1} = 0, 0.1, \dots, 1$ . Plot **c** ( $\gamma^{-1} = 1$ ) corresponds to a 3-photon NOON state displaying perfect super-resolving sinusoidal fringes. Remarkably, it turns out that increasing  $\gamma$ , i.e. attenuating the non-classical light, enables to selectively suppress certain peaks while leaving others almost unchanged. When the SPDC is completely blocked (plot **a**), the classical intensity phase dependence is obtained. Conveniently, most of the quantum narrowing is achieved with minute amounts of SPDC (plot **b**).

$$|\psi_3\rangle_{c,d} = \frac{\alpha}{4} \left( \frac{\alpha^2 - 3r}{\sqrt{3}} (|3,0\rangle_{c,d} + e^{3i\varphi} |0,3\rangle_{c,d}) + (\alpha^2 + r)(e^{i\varphi} |2,1\rangle_{c,d} + e^{2i\varphi} |1,2\rangle_{c,d}) \right) \quad (7)$$

After the two mode state is mixed again at the second BS we can consider the event of a 3 photon absorption in detector **f**:

$$|\langle 0,3|\psi_3\rangle_{e,f}|^2 = \frac{|\alpha|^2}{128} \left| \left( \frac{\alpha^2 - 3r}{\sqrt{3}} (1 - e^{3i\varphi}) + \sqrt{3}(\alpha^2 + r)(e^{2i\varphi} - e^{i\varphi}) \right) \right|^2 \quad (8)$$

The boundary cases here are of special interest; for a purely classical input ( $r = 0$ )

$$|\langle 0,3|\psi_3\rangle_{e,f}|_{\text{classical}}^2 = \frac{|\alpha|^6}{12} \sin^6\left(\frac{\varphi}{2}\right) \quad (9)$$

Indeed, 3-photon absorption of a classical interference pattern corresponds to the 3rd power of linear absorption phase dependence,  $\sin^2(\frac{\varphi}{2})$ . Equal amounts of quantum and classical light ( $\alpha^2 = -r$ ) would give here the 3-photon NOON state, which would have the following dependence on  $\varphi$ :

$$|\langle 0,3|\psi_3\rangle_{e,f}|_{\text{NOON}}^2 = \frac{|\alpha|^6}{6} \sin^2\left(\frac{3\varphi}{2}\right) \quad (10)$$

The width of the fringes in this case, matches that of classical light with a wavelength that is three times

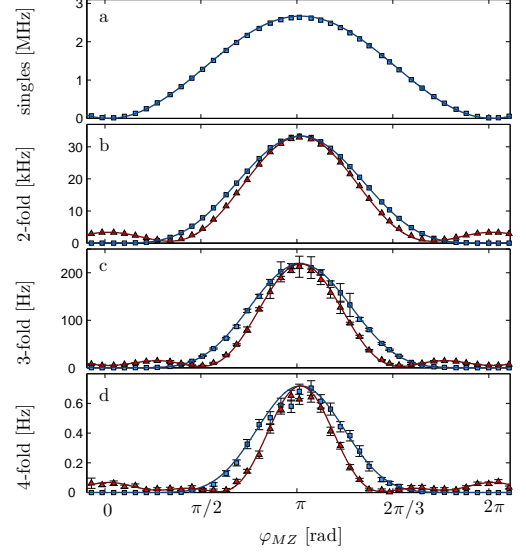


Figure 3: (color online). Experimental N-fold coincidence measurements for mixing SPDC and CS with a pair ratio of 1:10 ( $\gamma^{-1} = 0.1$ ) (**red triangles**) shown together with classical light only (**blue squares**). Solid lines are obtained from a simulation with no free parameters which takes into account the loss in the system and the detection efficiencies. **a** Classical single counts demonstrate classical resolution with a  $\sin^2(\frac{\varphi}{2})$  intensity dependence. Boxes **b-d** display number of  $|N\rangle_e |0\rangle_f$  events, i.e. N simultaneous “clicks” in detector **e**, with N=2-4 respectively. With only 10% of the quantum light required for a perfect NOON state, we create features with a width that scales like  $N^{-0.7}$ . In the 3-photon case, this amounts to 67% of the maximum possible narrowing, which is obtained with perfect NOON states.

shorter. The simulation in Fig.2 illustrates the intermediate cases. It displays the dependence of the 3-photon coincidence rate on the Mach Zehnder phase for different values of  $\gamma$ . Most importantly, the losses within the system and the efficiency of the detectors were taken into consideration. In particular, this amounts to accounting for the effect of higher coincidence orders on lower ones. The first plot (**a**), corresponding to the purely classical state (no SPDC), displays the classical  $\sin^6(\frac{\varphi}{2})$  dependence. As more quantum light is inserted into the system, the central peak becomes narrower and the plot gradually turns into the 3-photon NOON state (plot **c**). Remarkably, most of the narrowing effect of the central feature occurs at very low levels of SPDC. As an example of this, the case of  $\gamma^{-1} = 0.1$  is highlighted (plot **b**). In this example, 67% of the maximum possible narrowing, is achieved with only 10% of the quantum light required for creating perfect NOON states.

*Experimental setup and results.* The experimental setup is similar to the one described in [10] and is shown in Fig.1(B). Briefly, the scheme begins with generation of SPDC and coherent light with shared spatial and spec-

tral modes in perpendicular linear polarizations ( $\hat{H}, \hat{V}$ ). The relative phase between the beams is adjusted with a liquid crystal (LC) retarder after which they are overlapped on a polarizing beam splitter (PBS) cube. The phase shifter (PS) in the Mach-Zehnder (MZ) interferometer is implemented with the use of another LC oriented in  $45^\circ$  to the linear polarizations. This ensures phase stability in a co-linear, polarization based MZ. The two modes of the light are subsequently coupled into a polarization maintaining fiber which achieves the spatial mode matching. The output modes ( $\hat{H}, \hat{V}$ ) are separated by another PBS and detected by a photon number-resolving detection apparatus which is composed of an array of single-photon avalanche photodiodes.  $N$  photon events in port  $\hat{f}$  are measured as a function of the MZ phase ( $\varphi$ ). We preform this measurement for  $N = 1, 2, 3, 4$ , (Fig.3). For  $N \geq 2$ , the quantum result (at  $\gamma^{-1} = 0.1$ ) is shown together with the classical ( $\gamma^{-1} = 0$ )  $N$ -photon absorption. The additional narrowing due to the SPDC is clearly visible.

The simulation in Fig. 4 compares the performances of a  $\gamma^{-1} = 0.1$  state with those of a NOON state under various experimental conditions. It shows the phase dependence of the 3-fold coincidence under ideal experimental conditions for both the NOON state (A) and the  $\gamma^{-1} = 0.1$  state (D). The next row (B and E) shows that under conditions that greatly reduce efficiency, the detection rate is drastically attenuated but its phase dependence is unchanged provided that the input flux remains the same. Clearly, in order to render the 3-photon flux practical for multi-photon lithography, the input flux must be increased. The bottom row shows the two states under the same efficiency conditions but with higher input fluxes. The NOON state is distorted under these conditions as the approximations under which it was created are no longer valid (C), [11]. At the same time, the  $\gamma^{-1} = 0.1$  state remains essentially unchanged (F).

**Conclusion.** We conclude by saying that a major impediment of quantum lithography, due to which it was hitherto deemed impractical, comes from the limited intensity of quantum light sources. In the scheme demonstrated here only 10% of the photon pairs are of quantum origin (originally entangled) thus allowing high fluxes of photons.

Moreover, it is safe to presume that any multi-photon photo-resist that would allow in the future practical quantum lithography would absorb with an efficiency that is far from perfect, [5, 15], implying that detectable absorption rates would require an increased generating flux. While current schemes for creating NOON states are limited to low input fluxes, high flux loss-resistant states possess classical behavior in the sense that higher input fluxes effect mostly the intensity of the signal, not so much distorting its quality.

Financial support of this research by the ERC grant QUAMI, the Minerva Foundation, and the Crown Pho-

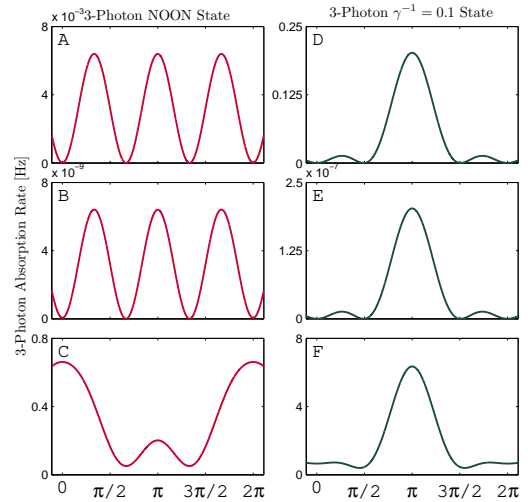


Figure 4: (color online). Simulation of 3-photon coincidence rates for NOON state (left column) and for a  $\gamma^{-1} = 0.1$  state (right column). The simulation takes into account losses in the system and imperfections in the quantum states due to high input photon flux. We define the setup transmission  $\eta$  as the ratio of the coincidences to singles in the SPDC, and the quantum flux  $N_p$  as the rate of pairs in the SPDC. The figures in the top row (A and D) show the ideal case in which the quantum states are flawless due to low photon flux ( $N_p = 10^{-6} \text{ Hz}$ ) and perfect transmission ( $\eta = 1$ ). The next row (B and E) illustrates the more practical case for lithography whereby the limited absorption of an  $N$ -photon resist would greatly reduce the efficiency ( $\eta = 0.01$ ). In this case, leaving the photon flux unchanged ( $N_p = 10^{-6} \text{ Hz}$ ) leads to virtually the same functional dependence at the cost of very low 3-photon detection rate. In order to reach a 3-fold coincidence rate which would be usable in practical lithography the flux must be substantially increased ( $N_p = 0.1 \text{ Hz}$ ) as shown in the last row (C and F). Since the approximation under which the NOON state was created is no longer valid at such fluxes it is completely deformed (C) while the  $\gamma^{-1} = 0.1$  state remains all but unharmed (F).

tonics Center is gratefully acknowledged.

- 
- [1] C. C. Gerry and P. L. Knight, *Introductory Quantum Optics* (Cambridge University Press, Cambridge, UK, 2005).
  - [2] A. N. Boto, P. Kok, D. S. Abrams, S. L. Braunstein, C. P. Williams, and J. P. Dowling, Phys. Rev. Lett. 85, 2733 (2000).
  - [3] G. Björk, L. L. Sa'nchez-Soto, and J. Söderholm, Phys. Rev. Lett. 86, 4516 (2001).
  - [4] P. Kok, A. N. Boto, D. S. Abrams, C. P. Williams, S. L. Braunstein, and J. P. Dowling, Phys. Rev. A 63, 063407 (2001).
  - [5] R. W. Boyd and J. P. Dowling, Quantum Inf Process (2011).
  - [6] J. P. Dowling, Contemp. Phys. 49 (2), 125-143 (2008).

- [7] M. W. Mitchell, J. S. Lundeen, and A. M. Steinberg, *Nature* 429, 161-164 (2004).
- [8] M. D'Angelo, M. V. Chekhova, and Y. Shih, *Phys. Rev. Lett.* 87, 013602 (2001).
- [9] P. Walther, J.-W. Pan, M. Aspelmeyer, R. Ursin, S. Gasparoni, and A. Zeilinger, *Nature* 429, 158-161 (2004).
- [10] I. Afek, O. Ambar, and Y. Silberberg, *Science* 328, 879 (2010).
- [11] H. F. Hofmann and T. Ono, *Phys. Rev. A* 76, 031806 (2007).
- [12] M. Kacprowicz, R. Demkowicz-Dobrzański, W. Wasilewski, K. Banaszek and I. A. Walmsley, *Nature Photonics* 4, 357 - 360 (2010).
- [13] G. S. Agarwal, K. W. Chan, R. W. Boyd, H. Cable, and J. P. Dowling, *J. Opt. Soc. Am. B* 24, 270-274 (2007).
- [14] F. Sciarrino, C. Vitelli, F. De Martini, R. Glasser, H. Cable, and J. P. Dowling, *Phys. Rev. A* 77, 012324 (2008).
- [15] M. P. Stocker, L. Li, R. R. Gattass and J. T. Fourkas, *Nature Chemistry* 3, 223-227 (2011).